A FAR ULTRAVIOLET PHOTOMETRIC CORRECTION FOR LRO LAMP.

Y. Liu[1], K. D. Retherford[2], T. K. Greathouse[2], U. Raut[2], K. E. Mandt[3], A. R. Hendrix[4], J. T. S. Cahill[3], G. R. Gladstone[2], C. Grava[2], A. F. Egan[5], D. E. Kaufmann[5], W. R. Pryor[6]; [1]Lunar and Planetary Institute/USRA, Houston, TX (liu@lpi.usra.edu), [2]Southwest Research Institute, San Antonio, TX, [3]Johns Hopkins University Applied Physics Laboratory, Laurel, MD, [4]Planetary Sciences Institute, Tucson, AZ, [5]Southwest Research Institute, Boulder, CO, [6]Central Arizona University, Coolidge, AZ

Introduction: The Lunar Reconnaissance Orbiter (LRO) Lyman Alpha Mapping Project (LAMP) provides global coverage of both nightside and dayside of the Moon in the far ultraviolet (FUV) wavelengths between 57 and 196 nm [1]. The nightside observations use roughly uniform diffuse illumination sources from interplanetary medium Lyman-α sky glow and UV-bright stars so that traditional photometric corrections are not appropriate. In contrast, the dayside observations use sunlight as the illumination source where bidirectional reflectance is measured. The bidirectional reflectance is dependent on the incident, emission, and phase angles as well as the soil properties. To compare the same area covered from multiple observations with different viewing geometries and to compare data taken from different instruments, photometric corrections are needed to normalize the reflectance as if it is measured in the same observation geometry.

In this study, we discuss the FUV wavelength dependence of the lunar phase curves as seen by the LAMP instrument in dayside data. Our preliminary results indicate that the reflectance in the FUV wavelengths decreases with the increasing phase angles. This is similar to the phase curve in the UV-visible wavelengths as studied by Hapke et al. [2] and Sato et al. [3] using the LRO Wide Angle Camera (WAC) data, among other visible-wavelength lunar studies. We report the derived Hapke parameters at FUV wavelengths for our study areas and the improved LAMP dayside maps after photometric correction.

LAMP FUV Phase Curve: The LRO LAMP instrument is a push-broom style FUV imaging spectrograph with a spectral resolution of 2 nm and standard spatial resolution of ~ 250 m/pixel. Nominally pointed nadir, LAMP provides repeated observation of the Moon, enabling accumulation of FUV signal and higher data quality over the regions of interest. LAMP data were radiometrically calibrated to give the radiance factor $I/F(i,e,g)$, the radiance relative to a perfectly diffusing Lambert surface illuminated and viewed normally. Then the I/F were divided by the Lommel-Seeliger function, $LS = \cos i/(\cos i + \cos e)$, to get the reduced reflectance, where LS is a common factor in the radiative transfer equation for the theoretical photometric functions of particulate media.

To further improve signal/noise, we use 10 nm bandpasses combining five bins in the normal 2 nm products and lower spatial resolution (i.e., 10 km/pixel as compared to the standard 250 m/pixel) such that more photon events can be captured at each pixel for a given wavelength. The reduced reflectances at 165 nm against phase angles for selected mare and highlands regions are shown in **Figure 1**. For both selected mare and highlands, the reflectances decrease with increasing phase angles.

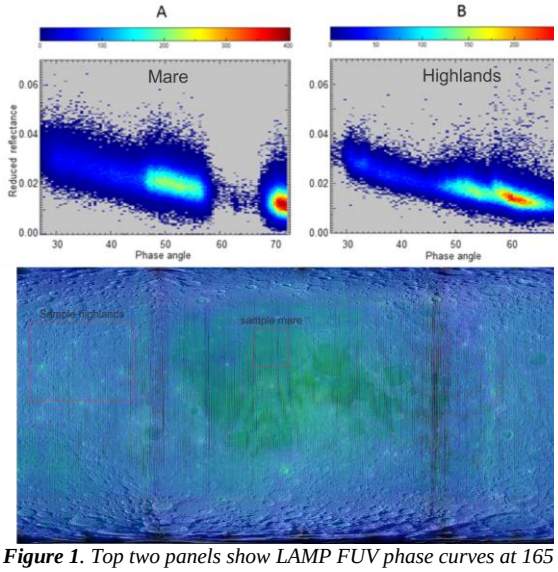

Figure 1*. Top two panels show LAMP FUV phase curves at 165 nm for selected mare and highlands regions. The points correspond to individual pixels that have varying albedos at the same angles. Colors in the dentisity plots indicate the number of data points used. Bottom panel is the LROC Wide Angle Camera (WAC) global mosaic of the Moon overlain by LAMP nightside Lyman alpha albedo maps with a transparency of 50%. The regions of interest are outlined by the red box.*

Simplified Hapke Model: The full theoretical function for the bidirectional reflectance is [4]:

$$r = K\frac{w}{4\pi}\frac{\mu_0}{\mu_0+\mu}\{[1+B_{S0}B_S(g)]p(g)+H(\mu_0)H(\mu)-1\}\cdot[1+B_{C0}B_C(g)]\cdot S(i,\,e,\,g) \quad (1)$$

This equation can be simiplified under many circumstances. Following *Hapke et al.* [2], we made several simplifications on modeling LRO LAMP data. For example, the porosity, *K*, was set to be 1 as it cannot be uniquely determined by remote sensing. The roughness parameter, *S*, was set to be 1 as the range of phase angles is insufficient to determine roughness. Additionally, we set the shadow hiding and coherent backscattering to be 0, as the phase angles are between 25° and 75° in our data so that opposition effects can be ig-

nored [2, 5]. Thus, the simplified Hapke bidirectional reflectance we used in this study is

$$r = \frac{w}{4\pi}\frac{\mu_0}{\mu_0+\mu}[p(g) + H(\mu_0)H(\mu) - 1] \quad (2)$$

Where *w* is single scattering albedo, *H* is multiple scattering function, and *p(g)* is one-term Henyey-Greenstein (HG) phase function which is expressed as

$$p(g) = \frac{1-b^2}{(1+2bcos(g)+b^2)^{3/2}} \quad (3)$$

The only unknown parameter, asymmetric factor *b*, in *p(g)* varies between -1 to 1 with negative values representing a backward scattering surface and positive values representing a forward scattering surface. Dividing the bidirectional reflectance by π and the Lommel-Seeliger function to give the reduced reflectance

$$r_{Reduce} = \frac{w}{4}[p(g) + H(\mu_0)H(\mu) - 1] \quad (4)$$

where r_{Reduce} is equivalent to the LAMP reflectance values plotted in Figure 1. Equation (4) only contains two free parameters, *w* and *b*.

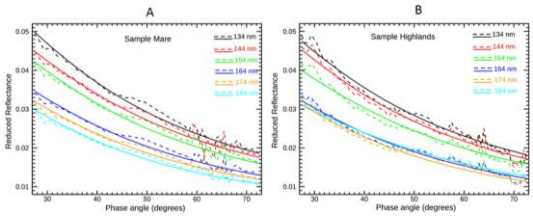

***Figure 2**. Reduced reflectance as a function of phase angles for the six wavelengths we modeled. The dashed lines are the running average (0.5 °wide) of the individual reduced reflectances. Solid lines are best fit using the simplified BRDF model of Hapke [2012]. (a) Fitting results for the mare region and (b) fitting results for the highland region.*

Results and Discussion: Equation (4) was fitted to the phase curves for the selected mare and highlands for each wavelength using Levenberg-Marquardt regression analysis algorithm. The example fitting results at wavelength 165 nm are shown in **Figure 2**, and the derived wavelength dependent single scattering albedo and asymmetric factor in the one-term HG phase function for the selected mare and highlands are listed in **Table 1**. The results show that the value of *w* decreases with wavelength, indicating bluer spectra of both regions at FUV wavelengths. The derived values for the asymmetry parameter *b* for the selected mare and highlands regions are all negative, indicating a strong backscattering of the lunar surface at FUV wavelengths. Using the derived photometric parameters, we performed photometric corrections on the LAMP FUV I/F data for the selected mare and highlands regions and normalized the reflectance with standard geometric angles. The normalized LAMP dayside albedo maps show significant improvement with photometric effects removed (**Figure 3**). Future work will include deriving spatially resolved global Hapke photometric parameter maps of the Moon at FUV wavelengths when more accumulated data are available.

Table 1. Retrieved wavelength dependent Hapke parameters for selected mare and highlands (*w* is the single scattering albedo, and *b* is the asymmetric factor in the single-particle phase function)

Wavelength (nm)		134	144	154	164	174	184
Mare	*w*	0.092± 0.002	0.084± 0.002	0.078± 0.002	0.064± 0.001	0.059± 0.001	0.055± 0.001
	b	-0.522± 0.016	-0.502± 0.015	-0.513± 0.014	-0.515± 0.014	-0.520± 0.013	-0.534± 0.014
Highlands	*w*	0.088± 0.002	0.083± 0.002	0.075± 0.002	0.060± 0.001	0.057± 0.001	0.060± 0.001
	b	-0.510± 0.017	-0.503± 0.018	-0.519± 0.016	-0.513± 0.015	-0.527± 0.014	-0.482± 0.014

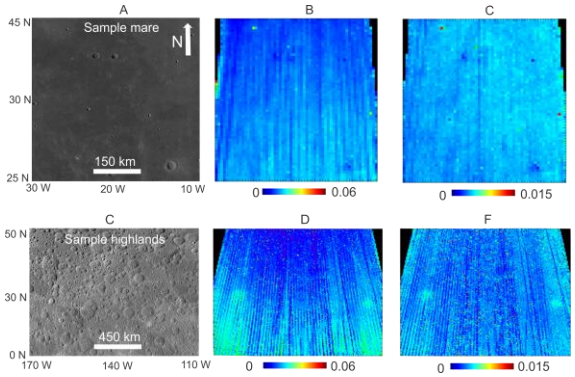

***Figure 3**. Comparison of reflectance at 165 nm before and after photometric corrections for selected mare and highlands regions. (a) WAC mosaic of the selected mare region, (b) the selected mare region before photometric correction, (c) the selected mare region after photometric correction, (d) WAC mosaic of the selected highlands region, (e) the selected highlands region before photometric correction, (f) the selected highlands region after photometric correction. These panels show that, after our photometric correction, the reflectance is more uniform across the entire scene for both regions. Equidistant cylindrical projection is applied for these maps.*

References: [1] Gladstone, G. R., et al. (2010), Space Sci. Rev., 150, 161-181. [2] Hapke, B., et al. (2012), J. Geophys. Res., 117, E00H15, doi:10.1029/2011JE003916. [3] Sato, H., et al. (2014), J. Geophys. Res. Planets, 119, 1775–1805, doi:10.1002/2013JE004580. [4] Hapke, B. (2012), Theory of Reflectance and Emittance Spectroscopy, 2nd ed., Cambridge Univ. Press, Cambridge, U. K. [5] Helfenstein, P., et al (1997), Icarus, 128, 2–14, doi:10.1006/icar.1997.5726.